Stress-relaxation due to crack–craze interaction

K. Sehanobish*, A. Chudnovsky† and A. Moet
Department of Macromolecular Science, Case Western Reserve University, Cleveland, OH 44106, USA
(Received 13 May 1992)

Stress-relaxation occurs in precracked polystyrene specimens accompanied by discontinuous crack growth under fixed displacement conditions. Crack growth is associated with a localized zone of dense crazes. The elliptically shaped craze zone increases in length as well as width with time. A model based on the double layer potential method of elastostatics is proposed to account for the drop in stress due to interactive crack–craze growth. This model successfully explains the observed non-linear stress-relaxation behaviour in terms of crack growth and crazing density.

(Keywords: polystyrene; stress-relaxation; craze; Green's tensor)

INTRODUCTION

As we continue to replace metals with plastics in structural components it is essential to consider the time-dependent performance of these materials. One can envisage situations where some of these components are going to be subjected to fixed boundary conditions. From our knowledge of viscoelasticity, we can only take the conventional stress-relaxation effect into design consideration. However, plastics may undergo irreversible deformation (crazing, shear banding, etc.) leading to crack initiation under such conditions. These processes can lead to additional stress-relaxation. This issue has been addressed in this paper using polystyrene as the model system.

Historically, stress-relaxation in amorphous polymers has been most extensively studied in solution or rubbery states. Several phenomenological models have been proposed involving Maxwell elements to account for the stress-relaxation behaviour of polymers. By appropriate combination of these elements, complex non-linear stress-relaxation behaviour can be simulated[1–4]. Subsequently, a deeper insight into the nature of relaxation processes has been sought using molecular models[5–7]. The molecular models proved extremely useful in solution and to some extent in the condensed rubbery state. In recent years, Matsuoka *et al.*[8] have extended these concepts to explain non-linear stress-relaxation in polymeric glasses close to their glass transition temperature. The authors suggest that under specific conditions the material might choose to relieve stresses by delayed crazing or even brittle fracture. More recently, models have been proposed based on Johnston–Gilman dislocation theory to estimate plastic deformation by homogeneous crazing in order to explain the nature of stress-relaxation and creep associated with crazing[9–11]. However, the presence of a macroscopic crack can further complicate the nature of stress-relaxation and creep. Although models for crack enhanced creep are available for metals and ceramics[12], no effort has been made to model crack enhanced creep in polymers[13].

In an earlier experimental study[14], discontinuous crack propagation associated with crazing has been observed under stress-relaxation. Using a double layer potential technique the amount of stress-relaxation due to crack–craze growth in polystyrene is estimated in this paper.

EXPERIMENTAL

The material used was plane isotropic extruded sheets (0.25 mm thick) of polystyrene obtained from Transilwrap Corporation (Cleveland, OH, USA). The draw ratio of the material was ~1.8 in two mutually perpendicular directions. Standard tensile tests showed that the Young's modulus (E) is ~2.2 GPa, the tensile fracture stress is ~60 MPa and the ultimate elongation over 60 mm gauge length is ~3.5%.

A straight notch of 4 mm depth was introduced into rectangular specimens (20 × 80) mm at a controlled rate using a razor blade fitted to an Instron crosshead. The edges were then carefully polished using metallographic techniques to a 0.3 μm final finish. Polished samples were subsequently conditioned by annealing at 90°C for 48 h followed by cooling slowly ($-10°C\,h^{-1}$) to room temperature.

The sample was monotonically loaded to initiate a crack at the notch tip and then held under fixed elongation in an Instron tensile testing machine. While crack growth and craze evolution were observed using a motor driven 35 mm camera attached to an optical microscope, stress-relaxation data were simultaneously recorded on a chart recorder. Stress-relaxation occurs in the sample for ~20 h eventually reaching an equilibrium value.

* To whom correspondence should be addressed. Present address: Dow Chemical Co., B-1218, Freeport, TX 77541, USA
† Present address: University of Illinois, Chicago, IL 60680, USA

0032-3861/93/061212-04

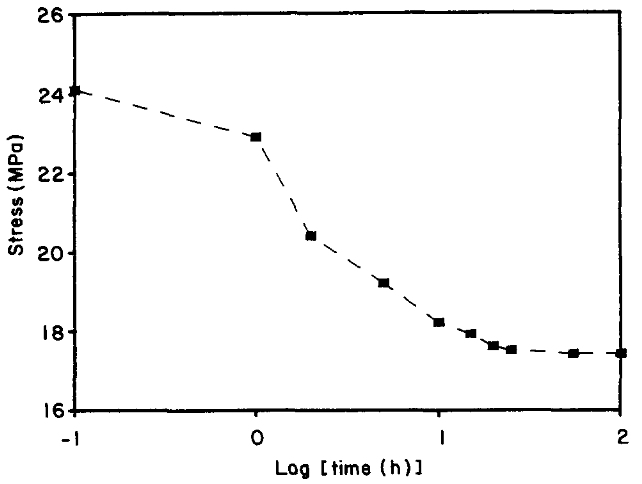

Figure 1 Semi-logarithmic plot of stress-relaxation behaviour of precracked polystyrene

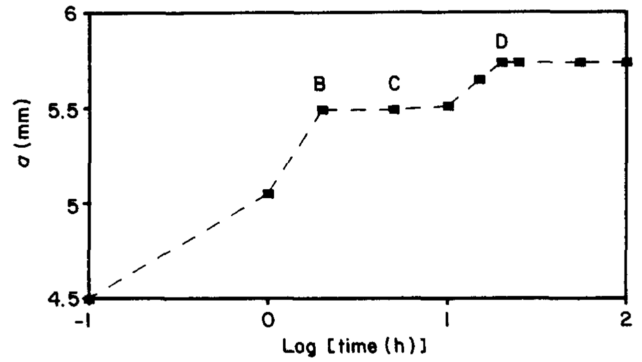

Figure 2 Plot of crack length *a versus* log time. Step BC corresponds to an intermediate crack arrest detected from kinetic measurements

RESULTS

Stress-relaxation behaviour of the precracked specimen is shown in *Figure 1*. Stress-relaxation occurs for ~20 h accompanied by discontinuous crack layer growth. The crack length is plotted in *Figure 2* as a function of logarithmic time. At the end of the first 2 h crack growth is abruptly arrested (BC in *Figure 2*) for the next 3 h. The crack then resumes its growth and stops again at 'D' after which no more crack propagation is observed for the next 80 h at which point the experiment is terminated. However, diffused surface crazes continue to appear throughout the sample. Significant stress-relaxation is observed during the entire history of crack propagation.

An optical micrograph representing a typical side view of the crack is shown in *Figure 3*. The crack propagates preceded and surrounded by a layer of dense crazes (crack layer). The elliptically shaped craze zone is characterized by its length l_a and width w. Both l_a and w increase monotonically with time (*Figures 4* and *5*), eventually attaining a constant value. This implies that the craze zone continues to evolve even when the crack remains arrested (BC in *Figure 2*).

DISCUSSION

The models proposed by Brown *et al.*[9,10] and Kitagawa and Kawagoe[11] can be applied to estimate stress-relaxation caused by homogeneous crazing. However, stress-relaxation may occur in association with localized crazing or with other damage mechanisms. It is therefore desirable to develop a model relating the time-dependent stress to the interactive crack–craze growth. The model proposed here takes into consideration stress-relaxation due to: the evolution of a non-homogeneous craze zone; crack growth; and interaction between the crack and the craze zone. The total displacement at the grips (Δ) is the sum of the displacements due to the bulk material (Δ_B),

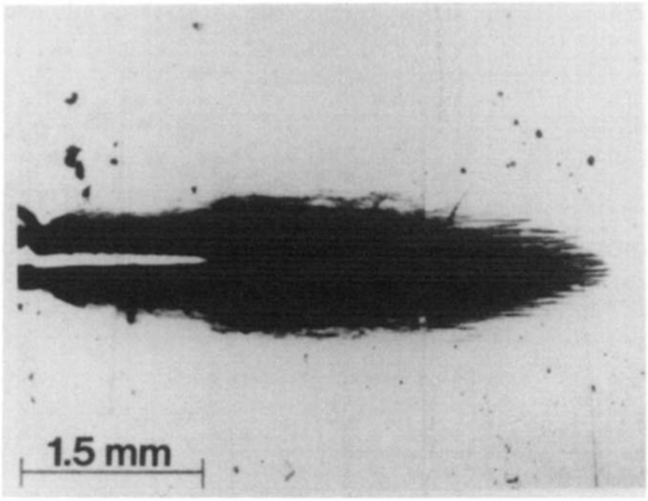

Figure 3 Optical micrograph displaying the crack and the crazed zone. The crazed zone is geometrically characterized by its length l_a and width w

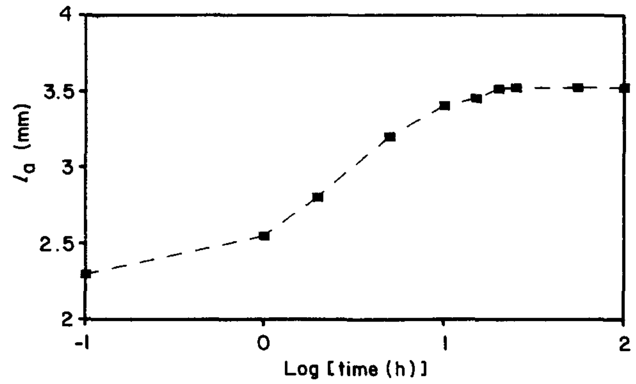

Figure 4 Evolution of the crazed zone length l_a as a function of log time

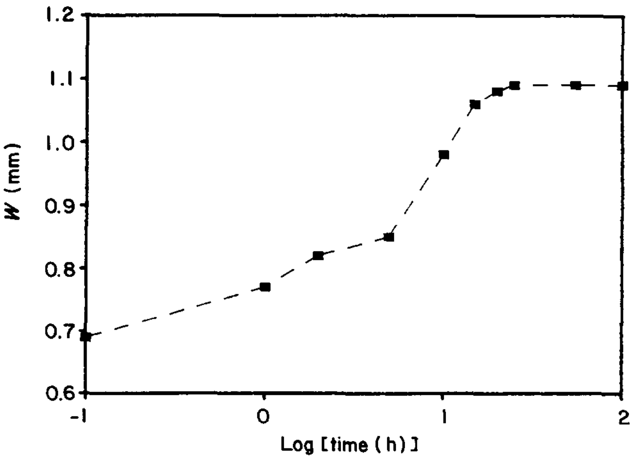

Figure 5 Evolution of the crazed zone width w as a function of log time

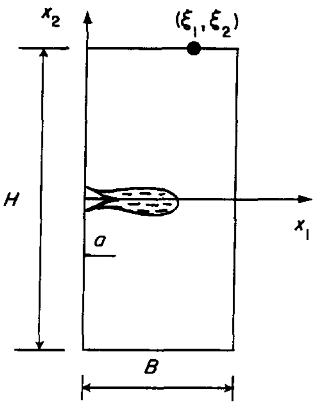

Figure 6 Schematic diagram of the specimen containing a crack layer within the chosen coordinate system. Coordinates (ξ_1, ξ_2) describe the location of a point on the grip of the specimen

the layer of crazes surrounding and preceding the crack tip (Δ_L) and the crack opening (Δ_C). Since the stiffness of the testing machine is considerably larger, the total displacement (Δ) is given by:

$$\Delta = \Delta_B + \Delta_L + \Delta_C \tag{1}$$

The displacement in the bulk material can be expressed using Hooke's law as:

$$\Delta_B = \frac{\sigma H}{E} \tag{2}$$

where σ is the stress applied to a specimen of original length H and E is Young's modulus.

In order to estimate displacements due to the crack (Δ_C) and due to the craze zone (Δ_L), the technique for double layer potential is employed. The potential theory thus employed is applicable to an isotropic elastic plane. The stress at any point, ξ, in an infinite elastic plane caused by the application of a unit force at another point, x, can be obtained by multiplying the unit force vector with a function $\varphi(x, \xi)$. The function, $\varphi(x, \xi)$, known as the second Green's tensor, transforms the unit force at one point to a traction vector at a different point. Applying the equilibrium equations for the medium, the second Green's tensor for the plane problem of elastostatics has been derived[15]. Since stresses and strains are linearly related in an elastic medium, the second Green's tensor can also be applied to obtain the displacement at a point x. In the case of a crack or a craze-like discontinuity, displacement occurs along the entire boundary. If this displacement distribution is described by a continuous function $b(x)$ over the entire length of the discontinuity, the double layer potential technique can be employed to determine the displacement at any point, ξ, due to jumps in displacements at the discontinuity. The function $b(x)$ can be referred to as the 'potential density'. The displacement field $u(x)$ due to a discontinuity (crack or craze) in an infinite elastic medium is expressed in the form of integrals of the potential density $b(x)$ multiplied by the second Green's tensor $\varphi(x, \xi)$ as:

$$u(x) = \int_d b(x)\varphi(x, \xi)\,dx \tag{3}$$

where d is the length of the discontinuity. The double layer potential method permits statistical averaging and requires a relatively simple computational routine.

A schematic diagram of the crack and the crazed layer is shown in *Figure 6*. The total displacement caused by a crazed layer is a sum of the displacements caused by individual crazes within the crazed zone. Hence, the displacement caused by the crazed layer at location ξ can be obtained by integrating over the entire volume of the crazed layer, V_L:

$$\Delta_L(\xi) = \int_{V_L} b(x)\varphi_{22}(x, \xi)\,dV_L \tag{4}$$

where $b(x)$ is the displacement caused by a single discontinuity (craze in the present case) at an arbitrary location, x, within the crazed zone. The vertical component of the second Green's tensor is derived as:

$$\varphi_{22}(x, \xi) = -\frac{(1+\nu)}{4\pi}\left\{\frac{(1-2\nu)(\xi_2 - x_2)}{(\xi_1 - x_1)^2 + (\xi_2 - x_2)^2} + \frac{2(\xi_2 - x_2)^3}{[(\xi_1 - x_1)^2 + (\xi_2 - x_2)^2]^2}\right\} \tag{5}$$

where ν is Poisson's ratio. The component of the influence tensor, $\varphi_{22}(x, \xi)$, acts as a linear operator transforming the jump in displacement at coordinate (x_1, x_2) to the resulting displacement at (ξ_1, ξ_2), at the grips. Finally, the average displacement at the grips can be evaluated by integrating over the width (B) of the specimen as:

$$\langle \Delta_L \rangle = \frac{2}{B}\int_0^B \Delta_L(\xi)\,d\xi \tag{6}$$

Assuming that the craze layer has an average craze density, $\langle \rho \rangle$ mm^2 of surfaces created per mm^3 volume, equation (4) can be simplified to:

$$\Delta_L = \langle \rho \rangle V_L \varphi_{22}(x_{1c}, x_{2c}) \tag{7}$$

where $\varphi_{22}(x_{1c}, x_{2c})$ is evaluated at the centre of gravity of the crazed layer. Geometric evaluation of the crazed zone recorded experimentally is then employed to compute the evolution of Δ_L from equations (6) and (7).

The displacement caused by the crack at the grips can similarly be calculated. However, in this case the integration is performed over the crack length a as:

$$\Delta_C = \int_a^b b(x)\varphi_{22}(x, \xi)\,dx \tag{8}$$

The displacement evaluated at location ξ is then averaged over the sample width B.

Since actual experimental results are used to calculate the displacements, (Δ_C, Δ_L), we do not need to account for the displacements due to crack–craze zone interaction and interactions between the individual crazes. It is quite obvious that both craze zone geometry and crack opening displacement are influenced by these interactions. Finally incorporating equation (1) into equation (2) and rearranging, we obtain the stress at the grips as:

$$\sigma(t) = \frac{(\Delta - \langle \Delta_C \rangle - \langle \Delta_L \rangle)E}{H} \tag{9}$$

Since the crack and the craze zone propagate, $\langle \Delta_C \rangle$ and $\langle \Delta_L \rangle$ in equation (9) increase with time, while the total displacement Δ remains fixed. Consequently, the stress $\sigma(t)$ at the grips decays. Assuming an average craze density $\langle \rho \rangle$ of 410 mm^2 mm^{-3} yields the best fit of the calculated solid line to the experimental stress-relaxation data (*Figure 7*). In an independent study on the same

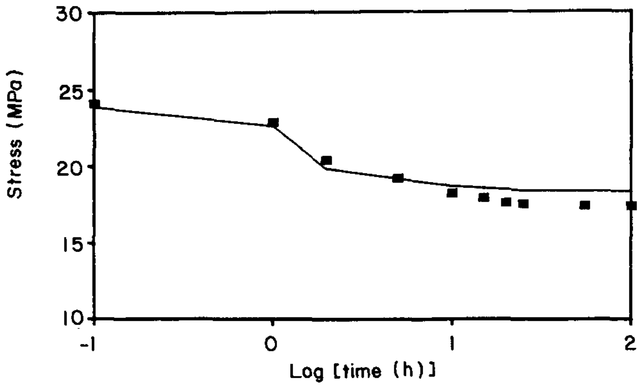

Figure 7 Comparison of the theoretical stress-relaxation behaviour (solid line) with the actual stress-relaxation data ($\langle\rho\rangle = 410\,mm^2\,mm^{-3}$)

material, thinned sections of the crazed zone were made and the actual craze density was estimated. The $\langle\rho\rangle$ assumed in the present calculations is well within the range of craze density reported in these investigations[16]. The observed discrepancy between the calculated and the experimental data past 20 h could probably be circumvented by considering the contribution due to surface crazes which continued to appear past 20 h. Since optical microscopic observations were focused at the crack tip region, no quantitative estimation of these surface crazes could be made.

CONCLUSIONS

A semi-empirical model is developed to account for stress-relaxation due to crack layer evolution. The model is based on the double layer potential technique which estimates displacement at any location in an elastic medium due to jumps in displacement at any other location. Predictions of this model are in reasonable agreement with the observed stress-relaxation behaviour. Thus, evolution of the crack layer under fixed displacement is responsible for the observed stress-relaxation.

REFERENCES

1 Kuhn, W. *Kolloid Z.* 1934, **68**, 2
2 Lederman, H. 'Elastic and Creep Properties of Filamentous Materials and Other High Polymers', Textile Foundation, Washington, 1943
3 Aleksandrov, A. P. and Lazurkin, Y. S. *J. Tech. Phys.* 1939, **9**, 1249
4 Ferry, J. D. 'Viscoelastic Properties of Polymers', Wiley, New York, 1970
5 Rouse Jr, P. E. *J. Chem. Phys.* 1953, **21**, 1272
6 Bueche, F. *J. Chem. Phys.* 1954, **22**, 603
7 Scott, K. W. and Stein, R. S. *J. Chem. Phys.* 1953, **21**, 1281
8 Matsuoka, S., Bair, H. E., Bearder, S. S., Kern, H. E. and Ryan, J. T. *Polym. Eng. Sci.* 1978, **18**, 1073
9 Wu, J. B. C. and Brown, N. *J. Soc. Rheol.* 1979, **23**, 231
10 Brown, N., Metzger, B. D. and Imai, Y. *J. Polym. Sci. A2* 1978, **16**, 1085
11 Kitagawa, M. and Kawagoe, M. *J. Mater. Sci.* 1979, **14**, 953
12 Hasselman, D. P. G. and Venkateswaran, A. *J. Mater. Sci.* 1983, **18**, 161
13 Kitagawa, M. and Motomura, K. *J. Polym. Sci. A2* 1974, **12**, 1979
14 Sehanobish, K., Baer, E., Chudnovsky, A. and Moet, A. *J. Mater. Sci.* 1985, **20**, 1934
15 Chudnovsky, A., Dolgopolsky, A. and Kachanov, M. NASA Report CR-172774, August 1984
16 Haddaoui, N., Chudnovsky, A. and Moet, A. *Polym. Mater. Sci. Eng.* 1983, **49**, 117